Hindawi
Mathematical Problems in Engineering
Volume 2023, Article ID 5564509, 14 pages
https://doi.org/10.1155/2023/5564509

Research Article

Soliton Solutions to the BA Model and (3 + 1)-Dimensional KP Equation Using Advanced $\exp(-\phi(\xi))$-Expansion Scheme in Mathematical Physics

HZ Mawa,[1] **S. M. Rayhanul Islam**,[2] **Md. Habibul Bashar**,[3] **Md. Mamunur Roshid**,[4] **Jahedul Islam**,[1] **and Sadia Akhter**[5]

[1]*Department of Civil Engineering, Presidency University, Dhaka 1212, Bangladesh*
[2]*Department of Mathematics, Pabna University of Science and Technology, Pabna 6600, Bangladesh*
[3]*Department of Mathematics, European University of Bangladesh (EUB), Dhaka 1216, Bangladesh*
[4]*Department of Mathematics, Bangladesh University of Engineering and Technology, Dhaka 1000, Bangladesh*
[5]*Department of Physics, Government Titumir College, Bir Uttam AK Khandakar Road, Dhaka 1213, Bangladesh*

Correspondence should be addressed to Md. Habibul Bashar; hbashar27.1273@gmail.com

Received 6 October 2023; Revised 24 October 2023; Accepted 28 October 2023; Published 21 November 2023

Academic Editor: Zhao Li

In this manuscript, the primary motivation is the implementation of the advanced $\exp(-\phi(\xi))$-expansion method to construct the soliton solution, which contains some controlling parameters of two distinct equations via the Biswas–Arshed model and the (3 + 1)-dimensional Kadomtsev–Petviashvili equation. Here, the solutions' behaviors are presented graphically under some conditions on those parameters. The height of the wave, wave direction, and angle of the obtained wave is formed by substituting the particular values of the considerations over showing figures with the control plot. With the collaboration of the advanced $\exp(-\phi(\xi))$-expansion method, we construct entirely the solitary wave results as well as rogue type soliton, combined singular soliton, kink, singular kink, bright and dark soliton, periodic shape, double periodic shape soliton, etc. Therefore, it is remarkable to perceive that the advanced $\exp(-\phi(\xi))$-expansion technique is a simple, viable, and numerical solid apparatus for clarifying careful outcomes to the other nonstraight equivalences.

1. Introduction

Nonlinear partial differential conditions (NLPDEs) are a critical subject and have spread broadly all over the planet in a wide range of dynamic designs. Numerous mathematicians and physicists are dissecting dynamic designs. Electrical conduction, plasma physics, mathematical natural sciences, fluid mechanics, optical fiber, solid-state physics, shallow water wave propagation, mathematical dynamics, and many other fields use dynamic structures as significant components of nonlinear physical simulations [1–10]. Recently, many experts looked into the optical soliton solutions of the NLPDEs. These solutions are essential for seeing how integrated physical phenomena work inside. For obtaining optical solutions for NLPDEs, numerous significant strategies have been proposed, including the modified polynomial expansion technique [11], the enhanced (G'/G)-expansion approach [12], the $\exp(-\phi(\xi))$-expansion technique [13], the generalized Kudryashov approach [14], the new auxiliary equation technique [15], the lie symmetry approach [16], the extended Fan subequation technique [17], the complex technique [18], the improved Bernoulli subequation approach [19], and so on.

Moreover, strength and bifurcation examination plays a significant role in figuring out how a nonlinear robust framework behaves. These days, numerous researchers have concentrated on the bifurcation examination of nonlinear differential conditions [20–29] to acquire significant knowledge of how nonlinear models behave and steadiness.

We have considered the two NLPDEs via the Biswas and Arshed (BA) and (3 + 1)-dimensional Kadomtsev–Petviashvili (KP) model in this manuscript. Many scholars have studied the BA and the (3 + 1)-dimensional KP models in the last few

decades and found many optical solutions. In its continuity, using two distinct schemes in [30, 31], they found the exact soliton solutions and the singular and dark solitons of the BA model with Kerr and power law in nonlinearity. The newly Φ^6-model expansion technique was applied to the BA model and attained the optical soliton solutions, representing the dark, bright, singular, rational, and periodic wave profile in [32]. In addition, it has been observed that some scholars have found the optical solution of the BA model using the trial solution technique [33], the modified simple equation approach [34], the mapping technique [35], and the extended trial function approach [36], which are dark, bright, singular, and periodic type wave profiles.

On the other hand, the $(3+1)$-dimensional KP model was first introduced in 1970 by Soviet physicists Kadomtsev and Petviashvili [37] which narrates the evolution of semi-one-dimensional shallow water waves while the effect of surface tension and viscosity is negligible. After that, many authors have studied the different forms of the KP model [38, 39]. Recently, one soliton and one resonant soliton solution have been found from the $(3+1)$-dimensional KP model using consistent tanh expansion [40]. Using the Bilinear method in [41], the KP model has explored the multiple lump solutions via 1-lump wave, 3-lump wave, 6-lump wave, and 8-lump waves. In addition, the simplified homogeneous balance method has been applied to the KP model and found the one single soliton and one double soliton solution in [42]. The Hirota bilinear transformation has been applied to the KP equation and obtained the one and two rough wave solutions in [43].

The purpose of the manuscript is to apply the advanced $\exp(-\phi(\xi))$-expansion approach [44, 45] to the BA model and the $(3+1)$-dimensional KP model, and to find some optical soliton solutions, namely w-shape, kink shape, periodic soliton solution shape, double periodic shape, dark soliton shape, combined singular soliton, and rogue wave profiles. Based on the above discussion in the previous literature, we can say that some wave profiles of the BA and $(3+1)$-dimensional KP models are new. Finally, it can perfect water rollers of extended wavelength with softly nonlinear repairing forces and regularity distribution. It can also be used to model waves in ferromagnetic media, nonlinear optics, optical fiber, and plasma physics.

The novelty of this paper is that, interestingly, the advanced $\exp(-\phi(\xi))$-extension approach is utilized for our concerned models concerning my insight. The impact of various norms of wave number on the got arrangements is likewise made sense of graphically. The acquired outcomes are helpful for the ultrashort light heartbeats in optical filaments. Our review model has much significance in quantum optics and liquid mechanics for making sense of the optical qualities of the femtosecond lasers and femtochemistry objects. Optical soliton annoyance is the foundation of the broadcast communications industry. This industry stays in business due to the wonder of soliton transmission innovation.

We have divided this article into follows: the literature review, objectives, and background are discussed in Section 1. We talked about the description of the tactic in Section 2. The governing equation is represented in Section 3. Section 4 applied the proposed method to the $(3+1)$-dimensional KP and BA model. Graphical and physical explanations have been discussed in Section 5. Finally, the conclusion is given in Section 6.

2. The Advanced $\exp(-\phi(\xi))$-Expansion Method

Section 2 consists of the summary of the advance $\exp(-\phi(\xi))$-expansion method [44, 45]. We consider the NLPDEs, which is of the form

$$R\left(U, U_x, U_y, U_t, U_{xx}, U_{xy}, U_{xt}, U_{yy}, U_{yt}, U_{tt}, \ldots\ldots\right), \tag{1}$$

where $U = U(x, y, t)$ is the wave function to be determined, R is a polynomial of $U(x, y, t)$, and its partial derivatives.

Step-1. First, we take a conversion variable to change all independent variables into a single variable, such as

$$U(x, t) = u(\eta), \quad \eta = kx + ly \pm Vt. \tag{2}$$

The wave variable mentioned in Equation (2) turn the NLPDE Equation (1) into an ODE as follows:

$$P\left(u, u', u'', \cdots \cdots \cdots\right) = 0. \tag{3}$$

Step-2. According to the advanced $\exp(-\phi(\xi)$-expanssion method, the exact solution of Equation (3) is assumed to be

$$u = \sum_{i=0}^{m} a_i \exp(-\phi(\xi))^i, \tag{4}$$

where $a_1, a_2, a_3 \ldots\ldots, a_m; a_m \neq 0,$ are constants to be determinted. The derivative of $\phi(\xi)$ satisfies the ODE in the succeeding system

$$\phi'(\xi) + A\exp(-\phi(\xi)) + B\exp(\phi(\xi)) = 0. \tag{5}$$

Then, the obtained results of ODE Equation (5) are of the hyperbolic, trigonometric, and the following forms:

Case I: hyperbolic function solution (when $AB < 0$):

$$\phi(\xi) = \ln\left(\sqrt{\frac{A}{-B}}\tan h\left(\sqrt{-AB}(\xi + C)\right)\right), \tag{6}$$

and

$$\phi(\xi) = \ln\left(\sqrt{\frac{A}{-B}}\coth\left(\sqrt{-AB}(\xi + C)\right)\right). \tag{7}$$

Case II: trigonometric function solution (when $AB>0$):

$$\phi(\xi) = \ln\left(\sqrt{\frac{A}{B}}\tan\left(\sqrt{AB}(\xi + C)\right)\right), \tag{8}$$

and

$$\phi(\xi) = \ln\left(-\sqrt{\frac{A}{B}}\cot\left(\sqrt{AB}(\xi + C)\right)\right). \tag{9}$$

Case III: when $B>0$ and $A=0$

$$\phi(\xi) = \ln\left(\frac{1}{-B(\xi + C)}\right). \tag{10}$$

Case IV: when $B=0$ and $A\in\mathbb{R}$

$$\phi(\xi) = \ln\left(A(\xi + C)\right), \tag{11}$$

where C is assimilating constants and $AB<0$ or $AB>0$ depends on sign of B.

Step-3. It is concerning the transformation of Equation (4) into Equation (3) and by combining all of the similar orders of $\exp(\phi(\xi))$ with the Equation (5). We obtain a polynomial form of $\exp(\phi(\xi))$. A collection of algebraic systems can be obtained by equating every coefficient of this polynomial to zero.

Step-4. Take up the approximation of the constants can be changed by measuring the mathematical terms come to be in Step 4. Replacing the approximations of the constants organized with the preparations of Equation (5), we will get new and extensive exact voyaging wave courses of action of the nonlinear advancement of Equation (1).

3. Governing Model

3.1. The BA Model. Recently, Biswas and Arshed [46] proposed a model with Kerr law nonlinearity, namely BA model is given as follows:

$$iq_t + a_1 q_{xx} + a_2 q_{xt} + i(b_1 q_{xxx} + b_2 q_{xxt}) = i[\rho(|q|^2 q)_x + T(|q|^2)_x q + \theta|q|^2 q_x]. \tag{12}$$

In Equation (12), the dependent variable $q(x, t)$ signifies the wave velocity that depends upon spatial (x) and temporal (t) variables. The first term portrays temporal evolution. a_1 and a_2 stand for the coefficient of GVD and spatiotemporal dispersion (STD); b_1 and b_2 represent third-order STD and third-order dispersion; A is the effect of self-steepening, B and ϑ are the effect of dispersions.

To start integration process, let

$$q(x,t) = U(\xi)e^{i\eta(x,t)}, \xi = x - vt, \eta(x,t) = -kx + \omega t + N, \tag{13}$$

where v, η, k, ω, and N are denoted by the amplitude portion of the wave, soliton speed, phase component, frequency, wave number, and phase constant, respectively. Next, put Equation (13) into Equation (12), the real part of Equation (12) has the following form:

$$(a_1 - a_2 v + 3b_1 k - 2b_2 vk - \omega b_2)U'' - (\omega + a_1 k^2 + b_1 k^3 - a_2 \omega k - b_2 \omega k^2)U = (\rho + \theta)kU^3, \tag{14}$$

and the imaginary part becomes

$$(b_2 vk^2 + 2b_2 \omega k - 3b_1 k^2 - v - 2a_1 k + 2a_2 vk + a_2 \omega)U' + (b_1 - b_2 v)U''' = (3\rho + 2T + \theta)U^2 U'. \tag{15}$$

3.2. The (3 + 1)-Dimensional KP Equation. Let us take into account the (3 + 1)-dimensional KP equation is in the following form:

$$(U_t + 6UU_x + U_{xxx})_x + 3U_{xx} + 3U_{zz} = 0. \tag{16}$$

The dependent variable $U(x, y, t)$ represents the wave velocity.

Using traveling wave variable $\xi = (\alpha x + \beta y + \gamma z - \omega t)$ to reduce the Equation (16) becomes

$$\alpha(-\omega U' + 6\alpha UU' + \alpha^3 U''')' + 3(\alpha^2 + \gamma^2)U'' = 0. \tag{17}$$

Equation (17) is an assimilated equation. Then assimilate two times with the help of ξ and we pursue the assimilating constant to zero. Then, we obtain

$$\alpha^4 U'' + 3\alpha^2 U^2 + (3\alpha^2 + 3\gamma^2 - \alpha\omega)U = 0, \tag{18}$$

where $U' = \frac{dU}{d\xi}$, $U'' = \frac{d^2U}{d\xi^2}$.

4. Applications

4.1. For BA Model. In this segment, we applied the advanced $\exp(-\phi(\xi))$-expansion method for Equations (14) and (15). Balancing the nonlinear terms and highest order derivative terms, we obtain the balance number $m = 2$ for Equations (14) and (15). So, the solution of the Equations (14) and (15) takes the following form:

$$U(\xi) = A_0 + A_1\exp(-\phi(\xi)) + A_2\exp(-\phi(\xi))^2. \tag{19}$$

Differentiating the Equation (19) with respect to ξ and putting the values of U, U', U'' and U''' in Equations (14) and (15), and equating the coefficient of $e^{i\phi(\xi)}$ $(i = 0, \pm1, \pm2....., \pm m)$ equal to zero.

Solving those systems of equivalences, we obtain the results for real part that is Equation (14) are as follows:

Set-1:

$$v = -\frac{1}{2}\frac{k^3b_1 - k^2\omega b_2 - 6kABb_1 + 2AB\omega b_2 + k^2a_1 - k\omega a_2 - 2ABa_1 + \omega}{AB(2kb_2 + a_2)}, \tag{20}$$

$$A_0 = 0, A_1 = \pm\sqrt{-\frac{-k^3Ab_1 + k^2A\omega b_2 - k^2Aa_1 + kA\omega a_2 - A\omega}{k\rho B + kB\theta}},\ A_2 = 0. \tag{21}$$

Case-I: we get the following hyperbolic solutions for $AB < 0$, yields

Family-1:

$$q_{1,2}(x,\ t) = \pm\frac{\sqrt{-\frac{-k^3Ab_1 + k^2A\omega b_2 - k^2Aa_1 + kA\omega a_2 - A\omega}{k\rho B + kB\theta}}}{\sqrt{-\frac{A}{B}}\tanh\left(\sqrt{-AB}(\xi + C)\right)} * e^{i\eta}, \tag{22}$$

$$q_{3,4}(x,\ t) = \pm\frac{\sqrt{-\frac{-k^3Ab_1 + k^2A\omega b_2 - k^2Aa_1 + kA\omega a_2 - A\omega}{k\rho B + kB\theta}}}{\sqrt{-\frac{A}{B}}\coth\left(\sqrt{-AB}(\xi + C)\right)} * e^{i\eta}, \tag{23}$$

where $\xi = x - vt$, $v = -\frac{1}{2}k^3b_1 - k^2\omega b_2 - 6kABb_1 + 2AB\omega b_2 + k^2a_1 - k\omega a_2 - 2ABa_1 + \omega/AB(2kb_2 + a_2)$, and $\eta(x,t) = -kx + \omega t + N$.

Case-II: we get the following trigonometric solutions for $AB > 0$, yields

Family-2:

$$q_{5,6}(x,\ t) = \pm\frac{\sqrt{-\frac{-k^3Ab_1 + k^2A\omega b_2 - k^2Aa_1 + kA\omega a_2 - A\omega}{k\rho B + kB\theta}}}{\sqrt{\frac{A}{B}}\tan\left(\sqrt{AB}(\xi + C)\right)} * e^{i\eta}, \tag{24}$$

$$q_{7,8}(x,\ t) = \mp\frac{\sqrt{-\frac{-k^3Ab_1 + k^2A\omega b_2 - k^2Aa_1 + kA\omega a_2 - A\omega}{k\rho B + kB\theta}}}{\sqrt{\frac{A}{B}}\cot\left(\sqrt{AB}(\xi + C)\right)} * e^{i\eta}, \tag{25}$$

where $\xi = x - vt$, $v = -\frac{1}{2}k^3b_1 - k^2\omega b_2 - 6kABb_1 + 2AB\omega b_2 + k^2a_1 - k\omega a_2 - 2ABa_1 + \omega/AB(2kb_2 + a_2)$, and $\eta(x,t) = -kx + \omega t + N$.

Case-III and Case IV: the values of A_0 and A_2 are not specified when $A = 0$. As a result, the outcome cannot be determined. This case is, therefore, dismissed. Essentially, when $B = 0$, the executing worth of A_0, A_1, and A_2 are undefined. So, they cannot be determined. So, this case was also discarded.

Again, we obtain the solutions for imaginary part that is Equation (15) we get following set

Set-2:

$$v=\frac{3k^2b_1-2k\omega b_2-2ABb_1+2ka_1-\omega a_2}{k^2b_1-2ABb_2+2ka_2-1},\ A_0=0,$$
$$A_1=\pm\sqrt{-\frac{12k^2b_1b_2-12k\omega {b_2}^2+12ka_1b_2-12ka_2b_1-6\omega a_2b_2+6b_1}{2Tk^2b_2-4TABb_2+3k^2\rho b_2+k^2\theta b_2-6AB\rho b_2-2AB\theta b_2+4Tka_2+6k\rho a_2+2k\theta a_2-2T-3\rho-\theta}}A, A_2=0. \tag{26}$$

Case-I: we get the following hyperbolic solutions when $AB<0$,

Family-3:

$$q_{9,10}(x,\ t)=\pm\frac{\Omega}{\sqrt{-\frac{A}{B}}\tanh\left(\sqrt{-AB}(\xi+C)\right)}*e^{i\eta}, \tag{27}$$

$$\Omega=\sqrt{-\frac{12k^2b_1b_2-12k\omega {b_2}^2+12ka_1b_2-12ka_2b_1-6\omega a_2b_2+6b_1}{2TK^2b_2-4TABb_2+3k^2\rho b_2+k^2\theta b_2-6AB\rho b_2-2AB\theta b_2+4Tka_2+6k\rho a_2+2k\theta a_2-2T-3\rho-\theta}}A, \tag{29}$$

$\xi=x-vt, v=\frac{3k^2b_1-2k\omega b_2-2ABb_1+2ka_1-\omega a_2}{k^2b_2-2ABb_2+2ka_2-1}$, and $\eta(x,t)=-kx+\omega t+N$.

Case-II: we get following trigonometric solution when $AB>0$,

Family-4:

$$q_{13,14}(x,\ t)=\pm\frac{\Omega}{\sqrt{\frac{A}{B}}\tan\left(\sqrt{AB}(\xi+C)\right)}*e^{i\eta}, \tag{30}$$

$$\Omega=\sqrt{-\frac{12k^2b_1b_2-12k\omega {b_2}^2+12ka_1b_2-12ka_2b_1-6\omega a_2b_2+6b_1}{2Tk^2b_2-4TABb_2+3k^2\rho b_2+k^2\theta b_2-6AB\rho b_2-2AB\theta b_2+4Tka_2+6k\rho a_2+2k\theta a_2-2T-3\rho-\theta}}A, \tag{32}$$

$\xi=x-vt, v=3k^2b_1-2k\omega b_2-2ABb_1+2ka_1-\omega a_2/k^2b_2-2ABb_2+2ka_2-1,$ and $\eta(x,t)=-kx+\omega t+N$.

$$q_{11,12}(x,\ t)=\pm\frac{\Omega}{\sqrt{-\frac{A}{B}}\coth\left(\sqrt{-AB}(\xi+C)\right)}*e^{i\eta}, \tag{28}$$

where

$$q_{15,16}(x,\ t)=\mp\frac{\Omega}{\sqrt{\frac{A}{B}}\cot\left(\sqrt{AB}(\xi+C)\right)}*e^{i\eta}, \tag{31}$$

where

Case-III: when $A=0$ the calculated value of A_0, A_1, and A_2 are undefined. So, the result cannot be determined. For this reason, this case is discarded.

Case-IV: when $B=0$ and $A\in\mathbb{R}$

$$q_{17,18}(x,t)=\pm\frac{\Omega}{(\xi+C)}*e^{i\eta}, \tag{33}$$

Family-5:

where

$$\Omega=\sqrt{-\frac{12k^2b_1b_2-12k\omega{b_2}^2+12ka_1b_2-12ka_2b_1-6\omega a_2b_2+6b_1}{2Tk^2b_2-4TABb_2+3k^2\rho b_2+k^2\rho b_2-6AB\rho b_2-2AB\theta b_2+4Tka_2+6k\rho a_2+2k\theta a_2-2T-3\rho-\theta}}A, \tag{34}$$

$\xi=x-\nu t, \nu=3k^2b_1-2k\omega b_2-2ABb_1+2ka_1-\omega a_2/k^2b_2-2ABb_2+2ka_2-1,$ and $\eta(x,t)=-kx+\omega t+N.$

4.2. For (3 + 1)-Dimensional KP Equation. In this segment, we apply the advance $\exp(-\phi(\xi))$-expansion approach for Equation (18) and since here the nonlinear term is U^2 and the highest order derivative is U''. So, the balance number is $m=2$. So, the solution of the Equation (18) takes Equation (19) and differentiates Equation (19) w. r. t. ξ and putting the values of U } and U'' in Equation (18) and equating the coefficient of $e^{i\phi(\xi)}$ $(i=0,\pm1,\pm2\ldots..,\pm m)$ equal to zero. Solving those systems of equations, we obtain the solutions for Equation (18), which are

Set-1:

$$\alpha=\alpha,\ \omega=-\frac{-4\alpha^4AB-3\alpha^2-3\gamma^2}{\alpha},\ A_0=-\frac{2}{3}\alpha^2AB,\ A_1=0, A_2=-2\alpha^2A^2. \tag{35}$$

Set-2:

$$\alpha=\alpha,\ \omega=-\frac{4\alpha^4AB-3\alpha^2-3\gamma^2}{\alpha},\ A_0=-2\alpha^2AB,\ A_1=0,\ A_2=-2\alpha^2A^2. \tag{36}$$

Case-I: we get following hyperbolic solutions when $AB<0$

Family-6:

$$U_{19}(x,\ t)=-\frac{2}{3}\alpha^2AB+\frac{2\alpha^2AB}{\tanh\left(\sqrt{-AB}(\xi+C)\right)^2}, \tag{37}$$

$$U_{20}(x,\ t)=-\frac{2}{3}\alpha^2AB+\frac{2\alpha^2AB}{\coth\left(\sqrt{-AB}(\xi+C)\right)^2}, \tag{38}$$

where $\xi=(\alpha x+\beta y+\gamma z-\omega t)$ and $\omega=-\frac{-4\alpha^4A\mu-3\alpha^2-3\gamma^2}{\alpha}$.

Family-7:

$$U_{21}(x,\ t)=-2\alpha^2AB+\frac{2\alpha^2AB}{\tanh\left(\sqrt{-AB}(\xi+C)\right)^2}, \tag{39}$$

$$U_{22}(x,\ t)=-2\alpha^2AB+\frac{2\alpha^2AB}{\coth\left(\sqrt{-AB}(\xi+C)\right)^2}, \tag{40}$$

where $\xi=(\alpha x+\beta y+\gamma z-\omega t)$ and $\omega=-\frac{4\alpha^4A\mu-3\alpha^2-3\gamma^2}{\alpha}$.

Case-II: we get following trigonometric solutions when $AB>0$,

Family-8:

$$U_{23}(x,\ t)=-\frac{2}{3}\alpha^2AB-\frac{2\alpha^2AB}{\tan\left(\sqrt{AB}(\xi+C)\right)^2}, \tag{41}$$

$$U_{24}(x,\ t)=-\frac{2}{3}\alpha^2AB-\frac{2\alpha^2AB}{\cot\left(\sqrt{AB}(\xi+C)\right)^2}, \tag{42}$$

where $\xi=(\alpha x+\beta y+\gamma z-\omega t)$ and $\omega=-\frac{-4\alpha^4A\mu-3\alpha^2-3\gamma^2}{\alpha}$.

Family-9:

$$U_{25}(x,\ t)=-2\alpha^2AB-\frac{2\alpha^2AB}{\tan\left(\sqrt{AB}(\xi+C)\right)^2}, \tag{43}$$

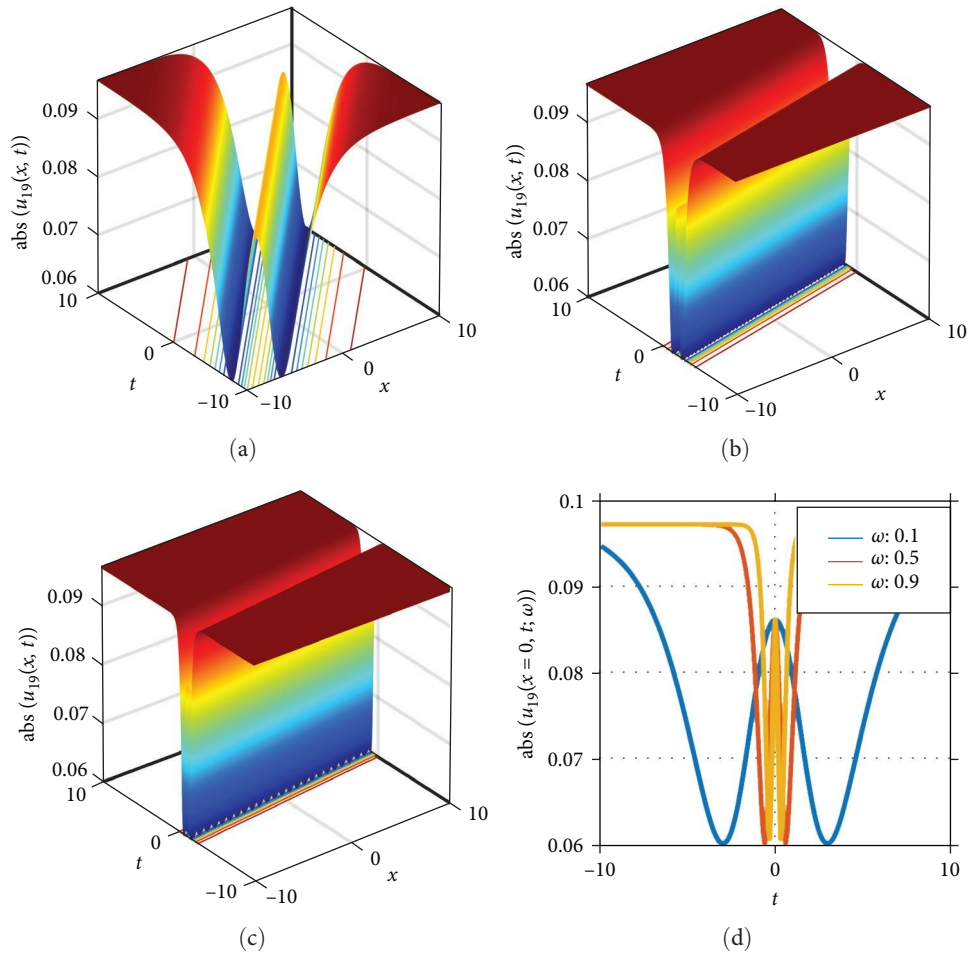

FIGURE 1: 3D (a–c) and 2D (d) plot of absolute part of the solution U_{19} when $A=-2, B=3, \alpha=0.11, C=\sqrt{-3}, z=0$ within the displacement $-10\le x, t\le 10$. (a) ω: 0.1, (b) ω: 0.5, and (c) ω: 0.9. abs, absolute.

$$U_{26}(x,\ t)=-2\alpha^2AB-\frac{2\alpha^2AB}{\cot\left(\sqrt{AB}(\xi+C)\right)^2}. \tag{44}$$

where $\xi=(\alpha x+\beta y+\gamma z-\omega t)$ and $\omega=-\frac{4\alpha^4A\mu-3\alpha^2-3\gamma^2}{\alpha}$.

Case-III and Case IV: the values of A_0 and A_2 are not specified when $A=0$. As a result, the outcome cannot be determined. This case is therefore dismissed. Essentially, when $B=0$ the executing worth of A_0 and A_1 are undefined. So, the result cannot be determined. For this reason, this case is discarded.

5. Physical and Graphical Explanations

This section will discuss the physical interpretation and graphical presentation of the $(3+1)$-dimensional KP and BA models that obtained exact and single-wave results. The precise traveling wave solutions for the $(3+1)$-dimensional KP equation and BA models can be obtained by utilizing the advanced $\exp(-\phi(\xi))$-expansion method. The arrangements $q_1, q_2, q_3, q_4, q_9, q_{10}, q_{11}, q_{12}, U_{19}, U_{20}, U_{21}$, and U_{22} are all hyperbolic function arrangements. The arrangements $q_5, q_6, q_7, q_8, q_{13}, q_{14}, q_{15}, q_{16}, U_{23}, U_{25}$, and U_{26} are all trigonometric function results, and the rational function arrangements being q_{17}, q_{18}.

According to the condition $AB<0$, the soliton solution U_{19} represents the w-shape wave profile for selecting the free parameters $A=-2, B=3, \alpha=0.11, C=\sqrt{-3}, z=0$ within the displacement $-10\le x, t\le 10$. The 3D plot with density plot wave features of the solution U_{19} depicted in Figure 1(a)–1(c) for the value of $\omega=0.1, 0.5, 0.9$, respectively. It can be seen that the wave propagates along the x- and t-axes. Figure 1(d) represents the 2D line plot of the U_{19} within displacement $-10\le t\le 10$. We need to observe the concave up and concave down of our desired sketch for the inflection point. By the observation, we find that $(-3, 0.09)$ at that point, the sketch shows the concave up to the concave down by the definition of inflection point we define that point.

According to the condition $AB<0$, imaginary form the of solution U_{20} which represents kink-shape with $A=-2, B=3, \alpha=.2, C=\sqrt{-2}, z=0$ within the displacements $-10\le x, t\le 10$. Figure 2(a)–2(c) represents a 3D plot with density

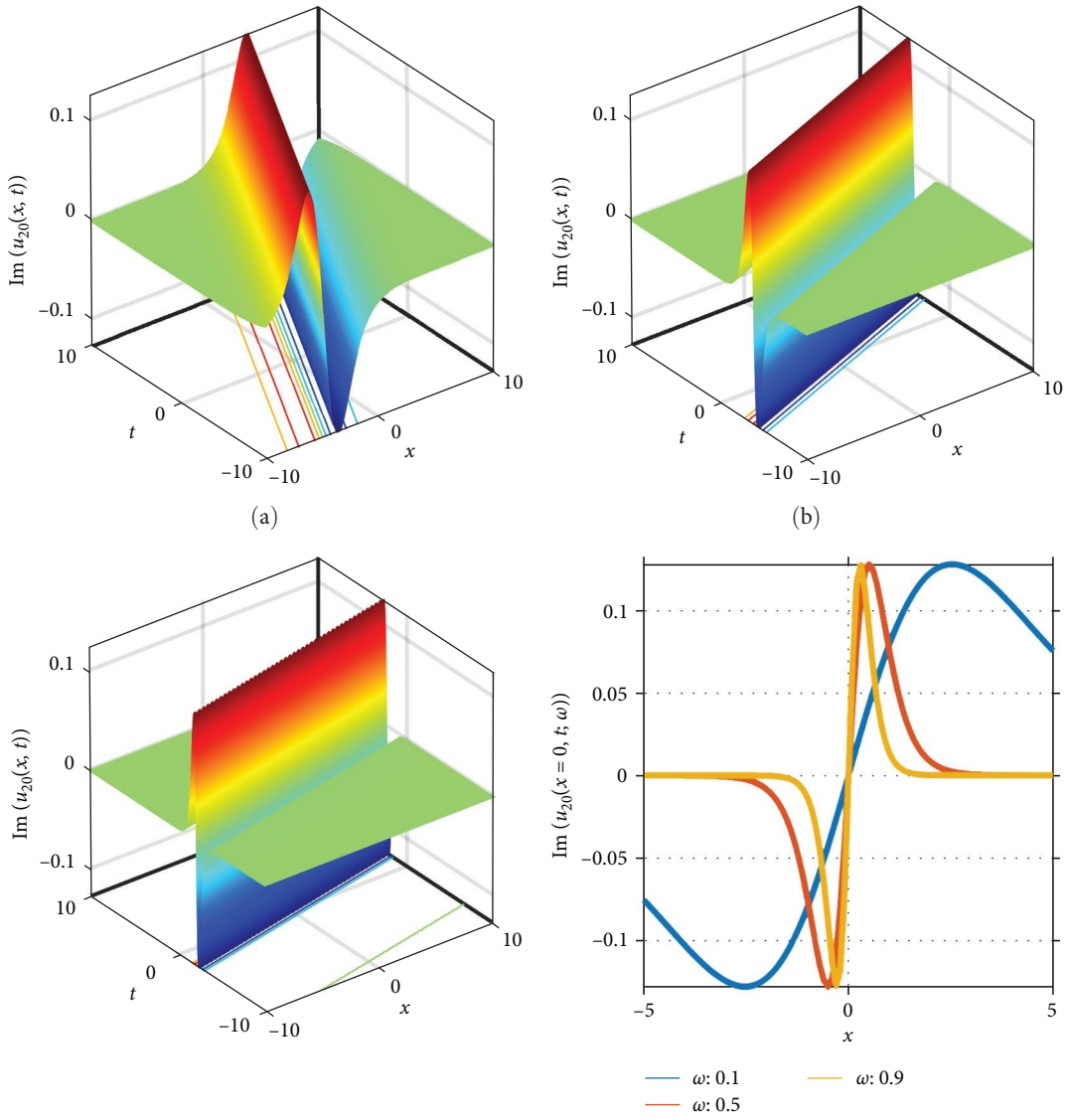

FIGURE 2: 3D (a–c) and 2D (d) plot of the complex part of solution U_{20} when $A = -2, B = 3, \alpha = .2, C = \sqrt{-2}, z = 0$ within the displacements $-10 \le x, t \le 10$. (a) $\omega: 0.1$, (b) $\omega: 0.5$, and (c) $\omega: 0.9$.

plot for the value of $\omega = 0.1, 0.5, 0.9$, respectively. Figure 2(d) indicates the 2D line plot of the U_{20} within displacement $-5 \le t \le 5$.

In the same way the solution U_{23} is a normal form and the sketch indicates in normal system, which represents in Figure 3. It indications the periodic soliton solution-shape type exact traveling wave solution $A = 3, B = 2, \alpha = 10, C = 2, z = 0$ within the displacements $-10 \le x \le 10$ and $-10 \le t \le 10$. Figure 3(a)–3(c) represents 3D plot with density plot for the value of $\omega = 0.1, 0.5, 0.9$, respectively. Figure 3(d) shows the 2D line plot of the U_{23} within displacement $-5 \le t \le 5$.

The solution q_9 is a complex form and the figure represents an imaginary form which represents in Figure 4. It spectacles the singular kink-shape type exact traveling wave solution with $A = -2, B = 3, b_1 = 1, b_2 = 1, a_1 = 2, a_2 = 1, k = 0.005, N = 1, C = 1, \theta = 11, p = \sqrt{-2}.2$ within the displacements $-10 \le x, t \le 10$. Figure 4(a)–4(c) represents 3D plot with density plot for the value of $\omega = 0.1, 0.5, 0.9$, respectively. Figure 4(d) shows the 2D line plot of the q_9 within displacement $-5 \le t \le 5$.

And the solution q_{11} is a complex form and the figure indicates in absolute system which represents in Figure 5. It shows the dark soliton-shape kind exact traveling wave solution with $A = -2, B = 3, b_1 = 1, b_2 = 1, a_1 = 2, a_2 = 1, k = 1, N = 1, C = 1, \theta = 1$ within the displacements $-20 \le x, t \le 20$. Figure 5(a)–5(c) represents 3D plot with density plot for the value of $\omega = 0.1, 0.5, 0.9$, respectively. Figure 5(d) indicates the 2D line plot of the q_{11} within displacement $-20 \le t \le 20$.

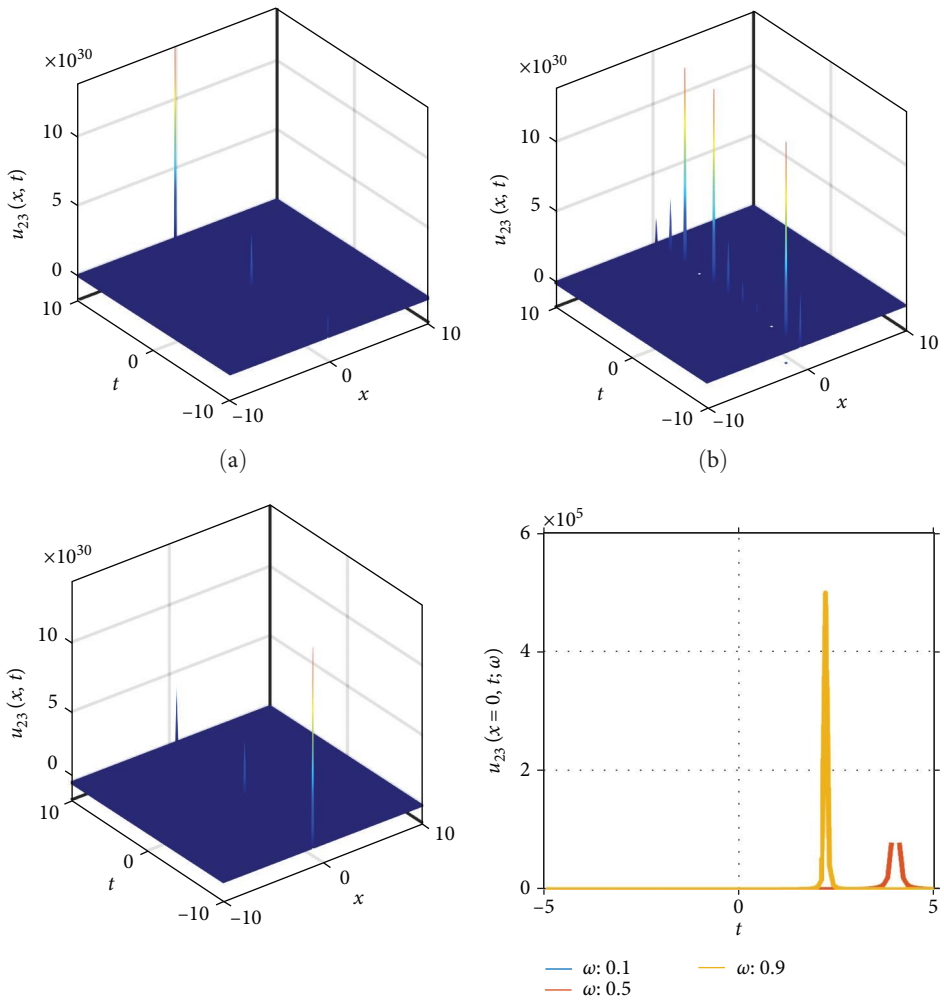

FIGURE 3: 3D (a–c) and 2D (d) plot of the solution of U_{23} when $A = 3, B = 2, \alpha = 10, C = 2, z = 0$ within the displacements $-10 \leq x \leq 10$ and $-10 \leq t \leq 10$. (a) $\omega : 0.1$, (b) $\omega : 0.5$, and (c) $\omega : 0.9$.

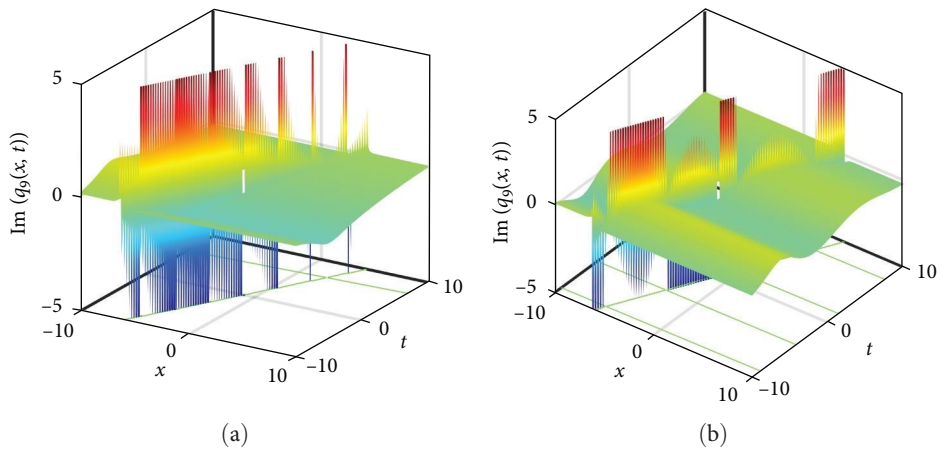

FIGURE 4: Continued.

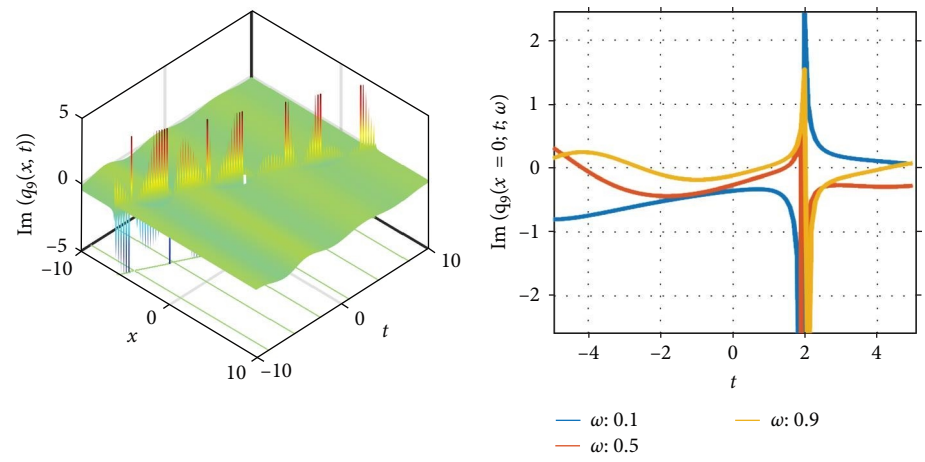

FIGURE 4: 3D (a–c) and 2D (d) plot of the complex part of solution q_9 when $A = -2, B = 3, b_1 = 1, b_2 = 1, a_1 = 2, a_2 = 1, k = .005, N = 1, C = 1, \theta = 11, p = \sqrt{-2}.2$ within the displacements $-10 \le x, t \le 10$. (a) $\omega : 0.1$, (b) $\omega : 0.5$, and (c) $\omega : 0.9$.

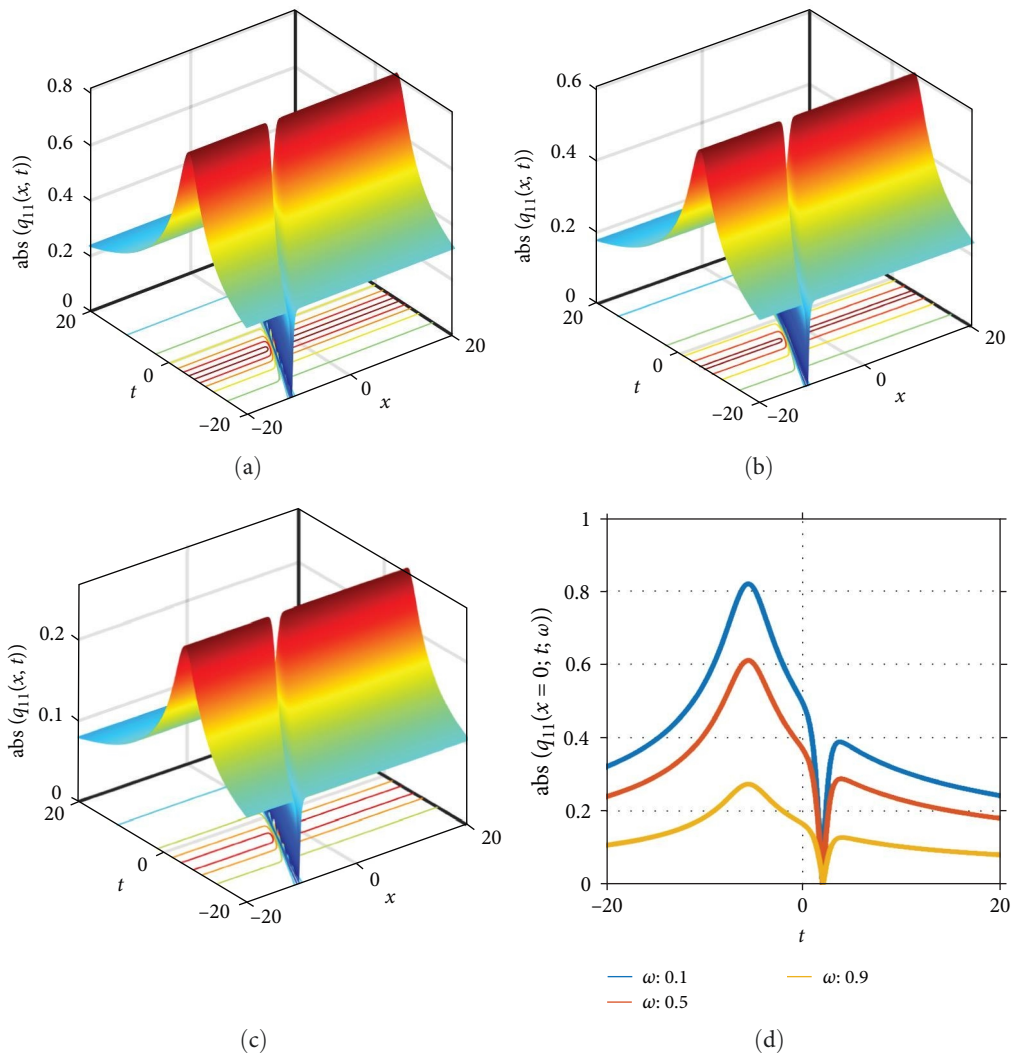

FIGURE 5: 3D (a–c) and 2D (d) plot of the absolute part of solution q_{11} when $A = -2, B = 3, b_1 = 1, b_2 = 1, a_1 = 2, a_2 = 1, k = 1, N = 1, C = 1, \theta = 1$ within the displacements $-20 \le x, t \le 20$. (a) $\omega : 0.1$, (b) $\omega : 0.5$, and (c) $\omega : 0.9$. abs, absolute.

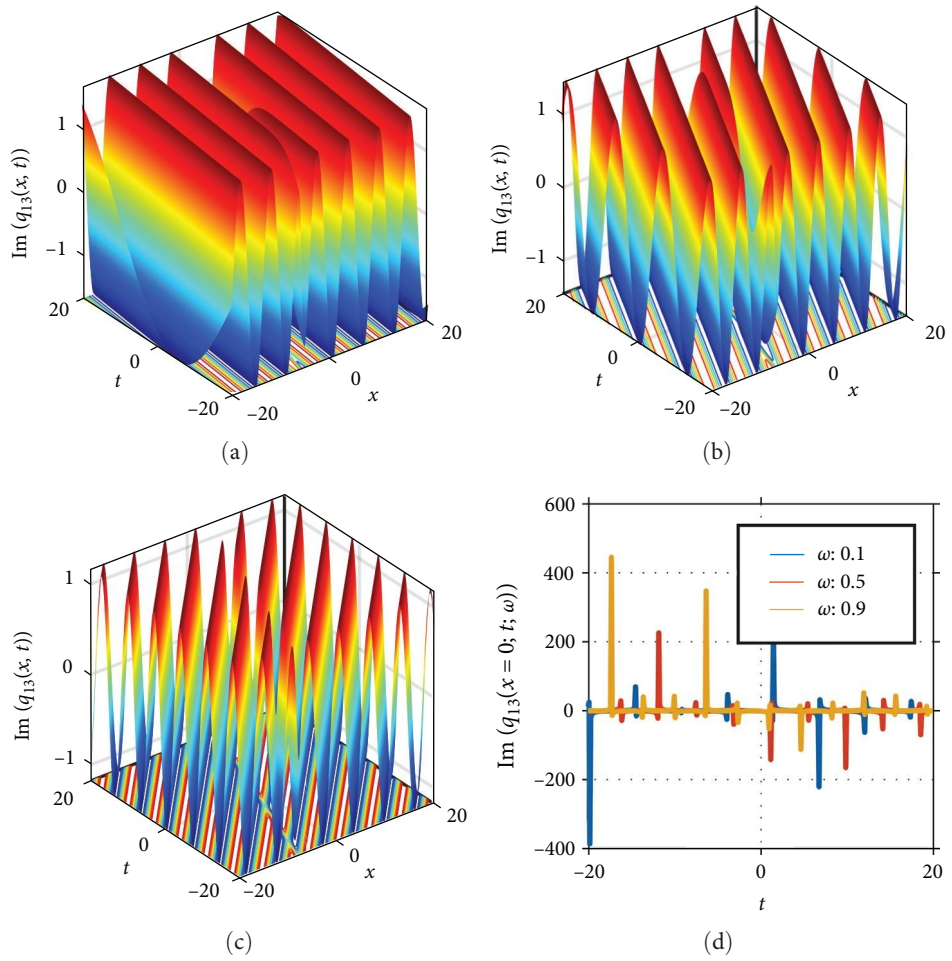

FIGURE 6: 3D (a–c) and 2D (d) plot of the complex part of solution q_{13} when $= 3, B = 2, b_1 = 1, b_2 = 1, a_1 = 2, a_2 = 1, k = 1, N = 1, C = 1, \theta = 1, T = 1, p = 1$ within the displacements and $-20 \leq x, t \leq 20$. (a) ω: 0.1, (b) ω: 0.5, and (c) ω: 0.9.

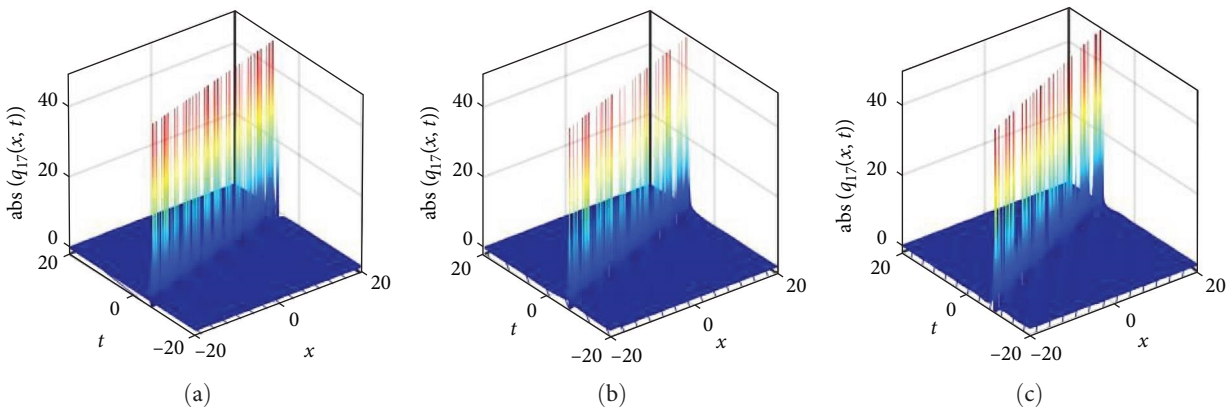

FIGURE 7: Continued.

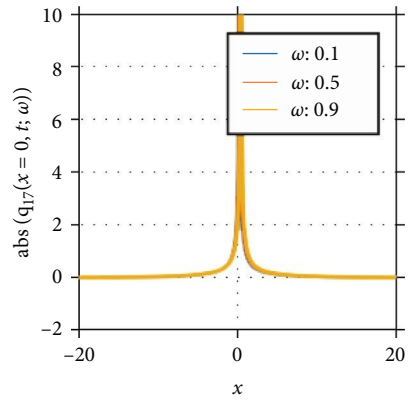

(d)

FIGURE 7: 3D (a–c)and 2D (d) plot of the absolute part of the solution q_{17} when $A = -2, B = 0, (\omega = 0.1, 0.5, 0.9), b_1 = 1, b_2 = 1, a_1 = 2, a_2 = 1, k = 1, N = 1, C = 1, \theta = 1/20, T = 1, p = 2$within the displacements $-20 \le x, t \le 20$. (a) ω:0.1, (b) ω:0.5, and (c) ω:0.9. abs, absolute.

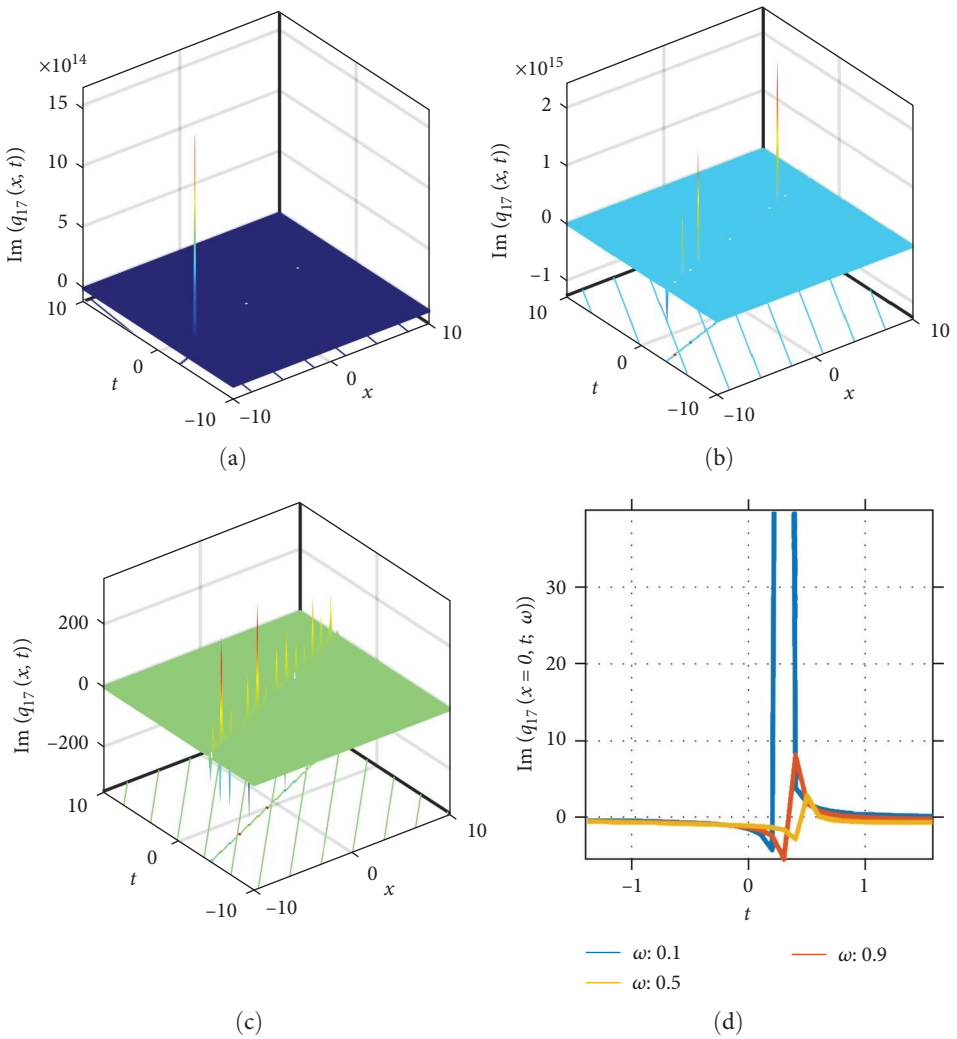

FIGURE 8: 3D (a–c) and 2D (d) plot of the complex part of the solution q_{17} when $A = -2, B = 0, (\omega = 0.1, 0.5, 0.9), b_1 = 1, b_2 = 1, a_1 = 2, a_2 = 1, k = 1, N = 1, C = 1, \theta = 1/20, T = 1, p = 2$ within the displacements $-20 \le x, t \le 20$. (a) ω:0.1, (b) ω:0.5, and (c) ω:0.9.

Again the solution q_{13} is a complex form and the figure in imaginary form which represents in Figure 6. Its expressions the double periodic-shape kind exact traveling wave solution with $A=3, B=2, b_1=1, b_2=1, a_1=2, a_2=1, k=1, N=1, C=1, \theta=1, T=1, p=1$within the displacements and $-20\le x, t\le 20$. Figure 6(a)–6(c) represents 3D plot with density plot for the value of $\omega=0.1, 0.5, 0.9$ respectively. Figure 6(d) indicates the 2D line plot of the q_{13} within displacement $-20\le t\le 20$.

Also the solution q_{17} is a complex form and sketch of absolute form and complex form represented in Figures 7 and 8. Figure 7 represents the combined singular soliton—shape. Figure 8 represents rouge kind shape with $A=-2$, $B=0$, $(\omega=0.1, 0.5, 0.9)$, $b_1=1, b_2=1, a_1=2, a_2=1, k=1, N=1, C=1, \theta=1/20, T=1, p=2$ within the displacements $-20\le x, t\le 20$ and also represents 2D line plot within displacement $-20\le t\le 20$.

6. Conclusion

This work explores the advanced $\exp(-\phi(\xi))$-expansion method successfully, and the significant shape solution is constructed with the controlling parameters. These solutions are elaborated systematically and graphically with 3D and 2D plots. Finally, it is found that the advanced $\exp(-\phi(\xi))$-expansion method to BA model and KP equation and such typical solutions might be beneficial to analyze and characterize many nonlinear phenomena in nonlinear optic, quantum field theory, solid state physics, and order to explain some intricate nonlinear physical phenomena, this method provides solutions with free parameters. This paper's solutions demonstrate that the approach is highly effective and adaptable.

Data Availability

No underlying data were collected or produced in this study.

Conflicts of Interest

The authors declare no conflict of interest.

Authors' Contributions

This paper was written with equal and significant contributions from all authors. All writers read and supported the last original copy.

References

[1] C. Coste, "Nonlinear Schrödinger equation and superfluid hydrodynamics," *The European Physical Journal Condensed Matter and Complex Systems*, vol. 1, no. 2, pp. 245–253, 1998.

[2] W. Yu, W. Liu, H. Triki, Q. Zhou, and A. Biswas, "Phase shift, oscillation and collision of the anti-dark solitons for the (3+1)-dimensional coupled nonlinear Schrödinger equation in an optical fiber communication system," *Nonlinear Dynamics*, vol. 97, no. 2, pp. 1253–1262, 2019.

[3] X. Y. Xie, B. Tian, W. R. Sun, M. Wang, and Y. P. Wang, "Solitary wave and multi-front wave collisions for the Bogoyavlenskii–Kadomtsev–Petviashili equation in physics, biology and electrical networks," *Modern Physics Letters B*, vol. 29, no. 31, Article ID 1550192, 2015.

[4] W. Liu, Y. Zhang, Z. Luan et al., "Dromion-like soliton interactions for nonlinear Schrödinger equation with variable coefficients in inhomogeneous optical fibers," *Nonlinear Dynamics*, vol. 96, no. 1, pp. 729–736, 2019.

[5] A. R. Seadawy, A. Ali, S. Althobaiti, and A. Sayed, "Propagation of wave solutions of nonlinear Heisenberg ferromagnetic spin chain and Vakhnenko dynamical equations arising in nonlinear water wave models," *Chaos, Solitons and Fractals*, vol. 146, Article ID 110629, 2021.

[6] S. M. R. Islam, K. Khan, and K. M. A. A. Woadud, "Analytical studies on the Benney–Luke equation in mathematical physics," *Waves in Random and Complex Media*, vol. 28, no. 2, pp. 300–309, 2018.

[7] S.-F. Tian, "Lie symmetry analysis, conservation laws and solitary wave solutions to a fourth-order nonlinear generalized Boussinesq water wave equation," *Applied Mathematics Letters*, vol. 100, Article ID 106056, 2020.

[8] A. R. Seadawy, D. Lu, and M. M. A. Khater, "Structure of optical soliton solutions for the generalized higher-order nonlinear Schrödinger equation with light-wave promulgation in an optical fiber," *Optical and Quantum Electronics*, vol. 50, no. 9, Article ID 333, 2018.

[9] S. M. R. Islam, "Application of an enhanced (G'/G)-expansion method to find exact solutions of nonlinear PDEs in particle physics," *American Journal of Applied Sciences*, vol. 12, no. 11, pp. 836–846, 2015.

[10] M. H. Bashar and S. M. R. Islam, "Exact solutions to the (2+1)-dimensional Heisenberg ferromagnetic spin chain equation by using modified simple equation and improve F-expansion methods," *Physics Open*, vol. 5, Article ID 100027, 2020.

[11] J. Lu, X. Duan, C. Li, and X. Hong, "Explicit solutions for the coupled nonlinear Drinfeld–Sokolov–Satsuma–Hirota system," *Results in Physics*, vol. 24, Article ID 104128, 2021.

[12] S. M. R. Islam, M. H. Bashar, and N. Muhammad, "Immeasurable soliton solutions and enhanced (G'/G)-expansion method," *Physics Open*, vol. 9, Article ID 100086, 2021.

[13] M. H. Bashar, S. M. R. Islam, and D. Kumar, "Construction of traveling wave solutions of the (2+1)-dimensional Heisenberg ferromagnetic spin chain equation," *Partial Differential Equations in Applied Mathematics*, vol. 4, Article ID 100040, 2021.

[14] M. Kaplan and A. Akbulut, "The analysis of the soliton-type solutions of conformable equations by using generalized Kudryashov method," *Optical Quantum Electronics*, 2021.

[15] M. H. Bashar, S. M. Y. Arafat, S. M. R. Islam, and M. M. Rahman, "Wave solutions of the couple Drinfel'd–Sokolov–Wilson equation: new wave solutions and free parameters effect," *Journal of Ocean Engineering and Science*, 2022.

[16] M. Devi, S. Yadav, and R. Arora, "Optimal system, invariance analysis of fourth-order nonlinear Ablowitz–Kaup–Newell–Segur water wave dynamical equation using lie symmetry approach," *Applied Mathematics and Computation*, vol. 404, Article ID 126230, 2021.

[17] K. U. Tariq, A. Zabihi, H. Rezazadeh, M. Younis, S. T. R. Rizvi, and R. Ansari, "On new closed form solutions: the (2+1)-dimensional Bogoyavlenskii system," *Modern Physics Letters B*, vol. 35, no. 9, Article ID 2150150, 2021.

[18] A. Majeed, M. Kamran, N. Asghar, and D. Baleanu, "Numerical approximation of inhomogeneous time fractional Burgers–Huxley equation with B-spline functions and Caputo derivative," *Engineering with Computers*, vol. 38, no. S2, pp. 885–900, 2022.

[19] A. Kumar, E. Ilhan, A. Ciancio, G. Yel, and H. M. Baskonus, "Extractions of some new travelling wave solutions to the conformable Date–Jimbo–Kashiwara–Miwa equation," *AIMS Mathematics*, vol. 6, no. 5, pp. 4238–4264, 2021.

[20] L. Tang, "Bifurcation analysis and multiple solitons in birefringent fibers with coupled Schrödinger–Hirota equation," *Chaos, Solitons and Fractals*, vol. 161, pp. 112383–112383, 2022.

[21] L. Tang, "Bifurcations and dispersive optical solitons for the nonlinear Schrödinger–Hirota equation in DWDM," *Optik*, vol. 262, pp. 169276–169276, 2022.

[22] L. Tang, "Bifurcations and dispersive optical solitons for the cubic-quartic nonlinear Lakshmanan–Porsezian–Daniel equation in polarization-preserving fibers," *Optik*, vol. 270, Article ID 170000, 2022.

[23] L. Tang, "Bifurcations and optical solitons for the coupled nonlinear Schrödinger equation in optical fiber Bragg gratings," *Journal of Optics*, vol. 52, no. 3, pp. 1388–1398, 2023.

[24] L. Tang, A. Biswas, Y. Yıldırım, and A. A. Alghamdi, "Bifurcation analysis and optical solitons for the concatenation model," *Physics Letters A*, vol. 480, pp. 128943–128943, 2023.

[25] L. Tang, "Bifurcation studies, chaotic pattern, phase diagrams and multiple optical solitons for the (2+1)-dimensional stochastic coupled nonlinear Schrödinger system with multiplicative white noise via Itô calculus," *Research Square*, vol. 1, 2023.

[26] Z. Li and C. Huang, "Bifurcation, phase portrait, chaotic pattern and optical soliton solutions of the conformable Fokas–Lenells model in optical fibers," *Chaos, Solitons & Fractals*, vol. 169, pp. 113237–113237, 2023.

[27] Z. Li and H. Hu, "Chaotic pattern, bifurcation, sensitivity and traveling wave solution of the coupled Kundu–Mukherjee–Naskar equation," *Results in Physics*, vol. 48, pp. 106441–106441, 2023.

[28] C. Peng and Z. Li, "Dynamics and optical solitons in polarization-preserving fibers for the cubic-quartic complex Ginzburg–Landau equation with quadratic–cubic law nonlinearity," *Results in Physics*, vol. 51, pp. 106615–106615, 2023.

[29] C. Peng and Z. Li, "Dynamic effects on traveling wave solutions of the space-fractional long-short-wave interaction system with multiplicative white noise," *Results in Physics*, vol. 53, pp. 106931–106931, 2023.

[30] M. Tahir and A. U. Awan, "Optical singular and dark solitons with Biswas–Arshed model by modified simple equation method," *Optik*, vol. 202, Article ID 163523, 2020.

[31] M. Tahir and A. U. Awan, "Optical traveling wave solutions for the Biswas–Arshed model in Kerr and non-Kerr law media," *Pramana-Journal of Physics*, vol. 94, no. 1, Article ID 29, 2020.

[32] N. Sajid and G. Akram, "Novel solutions of Biswas–Arshed equation by newly newly Φ^6-model expansion method," *Optik*, vol. 211, Article ID 164564, 2020.

[33] Y. Yildirim, "Optical solitons of Biswas–Arshed equation by trial equation technique," *Optik*, vol. 182, pp. 876–883, 2019.

[34] Y. Yildirim, "Optical solitons to Biswas–Arshed model in birefringent fibers using modified simple equation architecture," *Optik*, vol. 182, pp. 1149–1162, 2019.

[35] H. U. Rehman, M. S. Saleem, M. Zubair, S. Jafar, and I. Latif, "Optical solitons with Biswas–Arshed model using mapping method," *Optik*, vol. 194, Article ID 163091, 2019.

[36] M. Ekici and A. Sonmezoglu, "Optical solitons with Biswas–Arshed equation by the extended trial function method," *Optik*, vol. 177, pp. 13–20, 2019.

[37] B. B. Kadomtsev and V. I. Petviashvili, "On the stability of solitary waves in weakly dispersive media," *Soviet Physics Doklady*, vol. 15, pp. 539–541, 1970.

[38] W.-X. Ma and T. Xia, "Pfaffianized systems for a generalized Kadomtsev–Petviashvili equation," *Physica Scripta*, vol. 87, no. 5, Article ID 055003, 2013.

[39] A. M. Wazwaz, "Multi-front waves for extended form of modified Kadomtsev–Petviashvili equations," *Applied Mathematics and Mechanics*, vol. 32, no. 7, pp. 875–880, 2011.

[40] B. Ren, J. Yu, and X.-Z. Liu, "New interection solutions of (3+1)-dimensional KP and (2+1)-dimensional Boussinesq equations," *Abstract and Applied Analysis*, vol. 2015, Article ID 213847, 7 pages, 2015.

[41] L. He and Z. Zhao, "Multiple lump solutions and dynamics of the generalized (3+1)-dimensional KP equation," *Modern Physics Letters B*, vol. 34, no. 15, Article ID 2050167, 2020.

[42] Y. Xu, X. Zheng, and J. Xin, "New explicit and exact traveling wave solutions of (3+1)-dimensional KP equation," *Mathematical Foundations of Computing*, vol. 4, no. 2, pp. 105–105, 2021.

[43] Y.-L. Ma and B.-Q. Li, "Rogue wave solutions, soliton, and rough wave missed solution for a generalized (3+1)-dimensional Kadomtsev–Petviashvili equation in fluids," *Modern Physics Letters B*, vol. 32, no. 29, Article ID 1850358, 2018.

[44] N. H. M. Shahen, Foyjonnesa, M. H. Bashar, M. S. Ali, and A. A. Mamun, "Dynamical analysis of long-wave phenomena for the nonlinear confrmable space-time fractional (2+1)-dimensional AKNS equation in water wave mechanics," *Heliyon*, vol. 6, no. 10, Article ID e05276, 2020.

[45] M. H. Bashar, T. Tahseen, and N. H. M. Shahen, "Application of the advance $\exp(-\phi(\xi))$-expansion method to the nonlinear conformable time-fractional partial differential equations," *Turkish Journal of Mathematics and Computer Science*, vol. 13, pp. 68–80, 2021.

[46] A. Biswas and S. Arshed, "Optical solitons in presence of higher order dispersions and absence of self-phase modulation," *Optik*, vol. 174, pp. 452–459, 2018.